J Fluoresc (2011) 21:2193–2199
DOI 10.1007/s10895-011-0922-3

ORIGINAL PAPER

Study of Interaction of Silver Nanoparticles with Bovine Serum Albumin Using Fluorescence Spectroscopy

Jessy Mariam · P. M. Dongre · D. C. Kothari

Received: 20 December 2010 / Accepted: 4 July 2011 / Published online: 21 July 2011

Abstract The interaction between silver nanoparticles (SNPs) and Bovine Serum Albumin (BSA) was investigated at physiological pH in an aqueous solution using fluorescence spectroscopy. The analysis of fluorescence spectrum and fluorescence intensity indicates that SNPs have a strong ability to quench the intrinsic fluorescence of BSA by both static and dynamic quenching mechanisms. Resonance light scattering (RLS) spectra indicated the formation of a complex between BSA and SNP. The number of binding sites 'n' and binding constants 'K' were determined at different temperatures based on fluorescence quenching. The thermodynamic parameters namely ΔH°, ΔG°, ΔS° were calculated at different temperatures and the results indicate that hydrophobic forces are predominant in the SNP-BSA complex. Negative ΔG° values imply that the binding process is spontaneous. Synchronous fluorescence spectra showed a blue shift which is indicative of increasing hydrophobicity.

Keywords Silver nanoparticles · Bovine serum albumin · Fluorescence spectroscopy · Resonance light scattering

Introduction

Noble metallic nanoparticles are receiving increasing research attention in all fields of science in the past few decades due to their attractive physicochemical properties. Among the metallic nanoparticles, silver nanoparticles (SNPs) have received considerable attention because of their wide range of applications. Owing to their antibacterial activity, SNPs are proposed to be used to treat burn wounds [1], as coatings in surgical masks [2], in implantable devices [3] etc. SNPs have been used as biosensors to detect *E.coli* in apple and milk juice [4]. They have been used in conjunction with 9-aminoacridine an antitumor drug to study the antiproliferation effect on HeLa cells [5]. They are also known to exhibit antiplatelet properties in vivo which is useful in the treatment of thrombotic disorders. Anticoagulant and thrombolytic therapies for thrombotic disorders are usually associated with serious bleeding complications, and hence SNPs serve as potential antiplatelet/antithrombolytic agents as they do not confer any lytic effects on platelets [6].

However the introduction of SNPs in blood and their interactions with the proteins present in plasma is of central importance in biomedical applications of nanoparticles and the growing biosafety concerns of nanomaterials. The three dimensional structure assumed by a protein is unique and it can be considered to be thermodynamically most stable conformation adopted by the polypeptide chain. Albumins, the most abundant proteins in plasma, contribute to many important physiological functions like transport, buffer, nutrition etc. Thus any kind of conformational change in the protein can alter the function of the protein.

Therefore understanding the mechanisms of interaction of SNPs with BSA is of prime importance. BSA is the most abundant protein present in plasma. BSA has exceptional property to bind reversibly a huge number of compounds. BSA is the principal carrier of fatty acids, metabolic products like thyroxine, bilirubin, endogenous and exogenous compounds etc. The sulfhydryl groups present in BSA are scavengers of reactive oxygen and nitrogen species

J. Mariam · P. M. Dongre (✉)
Department of Biophysics, University of Mumbai,
Vidyanagari, Santacruz (E),
Mumbai 400 098, India
e-mail: drpmdongre@yahoo.co.in

D. C. Kothari
National Centre for Nanomaterials & Nanotechnology
and Department of Physics, University of Mumbai,
Vidyanagari, Santacruz (E),
Mumbai 400 098, India

which plays an important role in oxidative stress [7]. BSA has two tryptophan residues that possess intrinsic fluorescence. Trp 212 located within a hydrophobic binding pocket in the subdomain IIA and Trp 134, located on the surface of the albumin molecule in the first subdomain IB. The present investigation focuses on understanding the biophysical mechanisms of interactions between silver nanoparticles and BSA using fluorescence spectroscopy.

Experimental

Materials

Bovine Serum Albumin (SRL), silver nitrate (Qualigens) and trisodium citrate (SD, Fine) were used in this experiment. The stock solutions of BSA (10 mg/ml) were prepared in phosphate buffer of pH 7.4. The working solution of BSA was 1 mg/ml. All the chemicals were of analytical reagent grade and double distilled water was used throughout.

Methods

Synthesis and Characterization of SNPs

SNPs were synthesized by chemical reduction method. The synthesis procedure was a slightly modified form of Lee & Miesel [8]; hundred ml silver nitrate (10^{-3} $molL^{-1}$) was heated on a hot plate cum magnetic stirrer to 353 K; one percent trisodium citrate (50 ml) was added drop wise till the colorless solution turns yellow. The colour change indicates the formation of SNP. The number of silver atoms (N) in each silver nanoparticle is 31 d^3 where d is the size of the nanoparticle in nm [9]. Concentration of the silver nanoparticle solution is calculated using the equation:

$$C = \frac{N_{Total}}{NVN_A} \quad (1)$$

where N_{Total} is the total number of silver atoms added to the reaction solution-, N is the number of silver atoms present in each nanoparticle, V is the volume of the reaction solution in litres and N_A is the Avogadro's constant [10]. Using the above equation the concentration of silver nanoparticle was calculated to be 0.903×10^{-9} $molL^{-1}$. The colloidal silver nanoparticle solution was characterized using UV- visible (Implen nanophotometer). UV- visible absorption spectrum was recorded in the wavelength range of 200–600 nm using a one cm path length quartz cuvette. Dynamic light scattering (DLS) measurements were performed on Microtrac Inc particle size analyzer. Measurements were recorded at 298 K with an average of 3 runs.

UV-visible and Intrinsic Fluorescence Measurements

The UV-visible spectra of BSA and BSA in the presence of varying concentrations of SNPs were recorded in the wavelength range of 200–800 nm on Nanophotometer (Implen).

The fluorescence spectra were recorded in the wavelength range of 310–500 nm on Varian, Cary Eclipse fluorescence spectrophotometer using excitation wavelength of 295 nm. Fluorescence measurements were recorded at 277, 301, 310, 315 K. Excitation and emission slit widths were set at 10 nm and PMT voltage was set at 450 V. One cm pathlength rectangular quartz cuvette was used.

Resonance Light Scattering Spectra (RLS)

For Resonance Light Scattering Spectrum (RLS), the excitation and emission monochromators of the spectrofluorometer were scanned simultaneously (synchronous mode) in the wavelength range of 200–700 nm ($\Delta\lambda=0$ nm). Excitation and emission slit widths were set at 2.5 nm and PMT voltage was set at 450 V. RLS spectra were recorded after 30 min of incubation of SNP with BSA (0.2, 0.4, 0.6, 1 mg/ml). All the data were analyzed using the Cary Eclipse software.

Synchronous Fluorescence Spectra

In case of fluorescence synchronous scans, the initial excitation wavelength was set at 250 nm and scanned upto 500 nm, while the wavelength shift $\Delta\lambda$ was equal to 15 nm (for tyrosine residues) and 60 nm (for tryptophan residues).

Results and Discussion

Characterization of SNP

In the UV-visible spectrum (Fig. 1a) an absorption peak at 420 nm indicated the formation of SNP. DLS particle size distribution indicated an average particle size of 62 nm (Fig. 1b).

Absorption Characteristics of BSA-SNP

Figure 2 shows the absorption spectra of BSA and BSA in the presence of increasing concentration of SNP. From the figure it can be observed that as the quencher concentration increases, the intensity at the wavelength of 279 nm increases significantly with a blue shift of 2 nm. This increase in intensity can be attributed to the formation of the ground state complex between BSA and SNP, as BSA molecules get adsorbed on the surface of SNP.

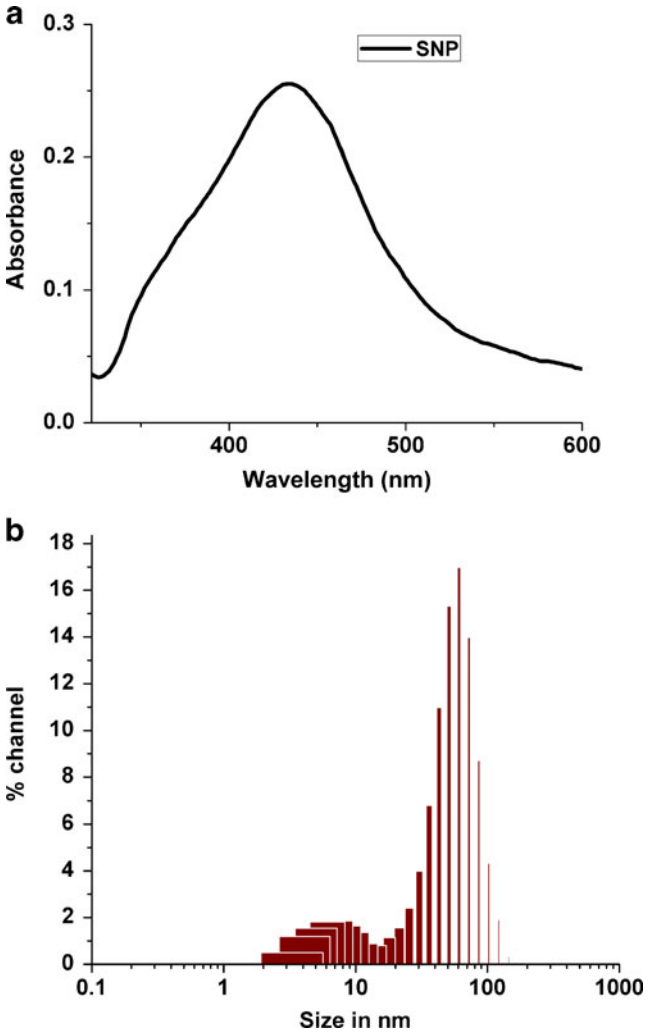

Fig. 1 **a** Absorption spectrum of silver nanoparticles. **b** Particle size distribution obtained from DLS measurements

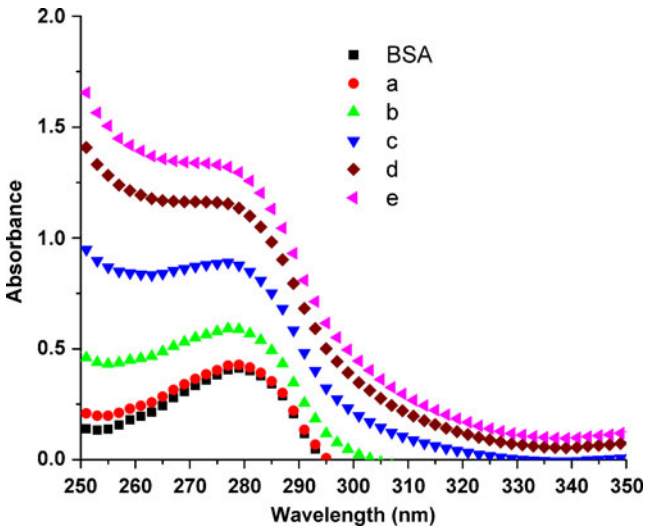

Fig. 2 UV- visible absorption spectra (*bottom* to *top*) of BSA and BSA in presence of 0.0903×10^{-9}, 0.225×10^{-9}, 0.451×10^{-9}, 0.677×10^{-9} and 0.8127×10^{-9} molL^{-1} SNP

The equilibrium for the formation of complex between BSA and SNP is given by Eq. 2,

$$\mathrm{BSA} + \mathrm{SNP} \overset{K_{app}}{\longleftrightarrow} \mathrm{BSA}\ldots\mathrm{SNP} \tag{2}$$

where K_{app} is the apparent association constant. The K_{app} value was calculated by the method reported by Benesi and Hildebrand [11] using Eq. 3

$$A_{obs} = (1-\alpha)C_0\varepsilon_{BSA}l + \alpha C_0\varepsilon_C l \tag{3}$$

where A_{obs} is the absorbance of the BSA solution containing different concentrations of SNP at 279 nm, α is the degree of association between BSA and SNP, ε_{BSA} and ε_C are the molar extinction coefficients at the defined wavelengths for BSA and the formed complex respectively, C_0 is the initial concentration of BSA and l is the optical pathlength.

Equation 3 can be expressed as Eq. 4

$$A_{obs} = (1-\alpha)A_0 + \alpha A_C \tag{4}$$

where A_0 and A_C are the absorbance of BSA and the complex at 279 nm respectively with the concentration of C_0. At relatively high SNP concentration, α can be equated to (K_{app} [SNP])/(1+ K_{app} [SNP]) where [SNP] is the concentration of silver nanoparticles in molL^{-1}. Thus Eq. 4 now becomes

$$\frac{1}{A_{obs}-A_0} = \frac{1}{A_C-A_0} + \frac{1}{K_{app}(A_C-A_0)[SNP]} \tag{5}$$

A graph of $1/(A_{obs}-A_0)$ versus 1/[Q] yielded a linear plot with a slope equal to $1/K_{app}$ (A_C-A_0) and an intercept equal to $1/(A_C-A_0)$. From this plot the value of K_{app} was calculated to be 1.58×10^9 Lmol^{-1}.

Characteristics of Fluorescence Spectra

Figure 3 shows the fluorescence emission spectra of BSA and BSA incubated with SNP upon excitation at 295 nm. It can be observed that as the concentration of SNP increases the emission intensity of BSA decreases gradually with a blue shift of around 5-6 nm. Similar results have been reported for the interaction of colloidal capped CdS nanoparticles with BSA [12].

Fluorescence quenching refers to any process that decreases the fluorescence intensity of a sample. A variety of molecular interactions can result in quenching. These include excited state reactions, molecular rearrangements, energy transfer, ground state complex formation and collisional quenching. Quenching can be induced by different mechanisms, which are usually classified into dynamic quenching and static quenching. Dynamic i.e. collisional quenching occurs when excited state fluorophore

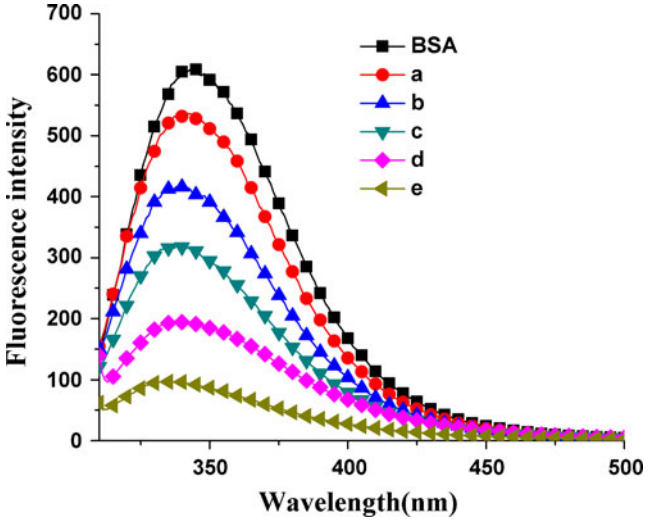

Fig. 3 Fluorescence spectra (*top* to *bottom*) of BSA & BSA in presence of SNP (a-e) concentrations of 0.0903×10^{-9}, 0.225×10^{-9}, 0.451×10^{-9}, 0.677×10^{-9} and 0.8127×10^{-9} molL^{-1}

is deactivated upon contact with the quencher molecule in solution. In this case the fluorophore is returned to the ground state during a diffusive encounter with the quencher. Static quenching occurs due to the formation of a nonfluorescent ground state complex between the fluorophore and the quencher. Dynamic and static quenching can be distinguished by their differing dependence on temperature. Higher temperature results in faster diffusion and larger amounts of collisional quenching and will typically lead to the dissociation of weakly bound complexes and smaller amounts of static quenching. The quenching constant increases with increasing temperature for dynamic quenching, however, it decreases with increasing temperature for static quenching [13].

The quenching data can be described by the Stern–Volmer equation [13]

$$F_0/F = 1 + k_q\tau_0[Q] = 1 + K_{SV}[Q] \quad (6)$$

where F_0 and F represent the fluorescence intensities in the absence and presence of quencher, k_q is the bimolecular quenching rate constant, K_{SV} is the Stern volmer constant, τ_0 is the average lifetime of the molecule without quencher and $[Q]$ is the concentration of the quencher. Attenuation of fluorescence intensities occur due to absorption of the incident light or absorption of the emitted light and hence fluorescence intensities were corrected for these inner filter effects using the relationship [13]

$$F_{corr} = F_{obs} \times e^{\frac{A_{ex}+A_{em}}{2}} \quad (7)$$

where F_{corr} and F_{obs} are the corrected and observed fluorescence intensities respectively, and A_{ex} and A_{em} are the absorption of the systems at the excitation and emission wavelengths respectively. Quenching data are usually presented as plots of F_o/F versus [Q]. This is because F_o/F is expected to be linearly dependent upon the concentration of the quencher. A plot of F_o/F versus [Q] yields a slope equal to stern volmer quenching constant. A linear Stern–Volmer plot is generally indicative of a single class of fluorophores, all equally accessible to the quencher. In many cases, the fluorophore can be quenched both by collision and by complex formation with the same quencher. When this is the case, the Stern–Volmer plot exhibits upward curvature, concave toward the *y*-axis at high [*Q*] [13].

The present investigation shows that both dynamic and static quenching were involved as demonstrated by the fact that the Stern–Volmer plot deviated from linearity toward the y-axis from the concentration 0.677×10^{-9} molL^{-1} of SNP (Fig. 4) (see for example ref 13). In the linear range of the Stern–Volmer regression curves the Stern volmer quenching constants for SNP were calculated. The values of K_{SV} at different temperatures are shown in Table 1.

Since the fluorescence lifetime of a biopolymer is 10^{-8} s [13], the k_q values were calculated using the formula $k_q = K_{SV}/\tau_o$. In case of dynamic quenching the maximum scatter quenching collision constant of various quenchers with the biopolymer is near 1×10^{10} Lmol^{-1}s^{-1} [13]. From the Table 1 it can be observed that k_q values are in the order of 10^{17} M^{-1}s^{-1}. This indicates that quenching is partly static in nature. K_{SV} values increase with increasing temperature, thus implying that partly the process may be dynamic. Thus the values of K_{SV} and k_q confirm our conclusion from Stern Volmer plot that BSA is quenched by mixed static and dynamic quenching mechanisms.

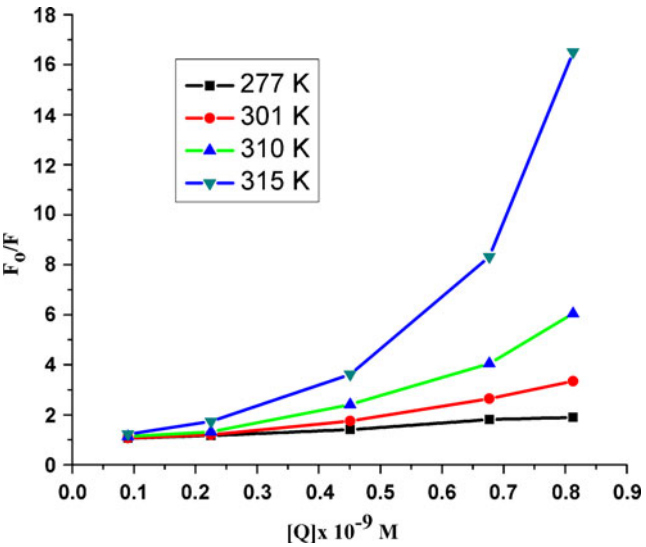

Fig. 4 Stern Volmer plot for SNP & BSA

Table 1 Stern-Volmer quenching constants for the interaction of SNPs with BSA at different temperatures

Temperature (K)	K_{SV} ($\times 10^{-9}$ M^{-1})	k_q (M^{-1} s^{-1})
277	1.27	1.82×10^{17}
301	2.70	3.27×10^{17}
310	5.06	3.63×10^{17}
315	11.9	6.46×10^{17}

Resonance Light Scattering Technique

It is a simple technique that allows easy detection of aggregates using a common spectrofluorimeter. Figure 5 shows the RLS spectra of BSA, SNP and mixture of BSA and SNP. BSA has a very weak RLS signal over the entire wavelength range of 200–700 nm [14] and SNP shows a peak at 462 nm (Fig. 5). However strong RLS signals (Fig. 5) can be observed in the mixtures of BSA and SNP with a maximum peak around 490 nm and a secondary one at 327 nm. RLS signals were found to increase with increasing concentration of protein. The production of RLS spectra is correlated with the formation of aggregates and the RLS intensity is dominated primarily by the dimensions of the aggregate formed in solution. It is inferred from the results that the added BSA may interact with SNP in solution, forming a new BSA-SNP complex that would be expected to be an aggregate. The dimensions of the resultant BSA-SNP complex should be larger than that of BSA and may be much less than the incident wavelength, due to which enhanced light scattering is occurring under the given conditions [15].

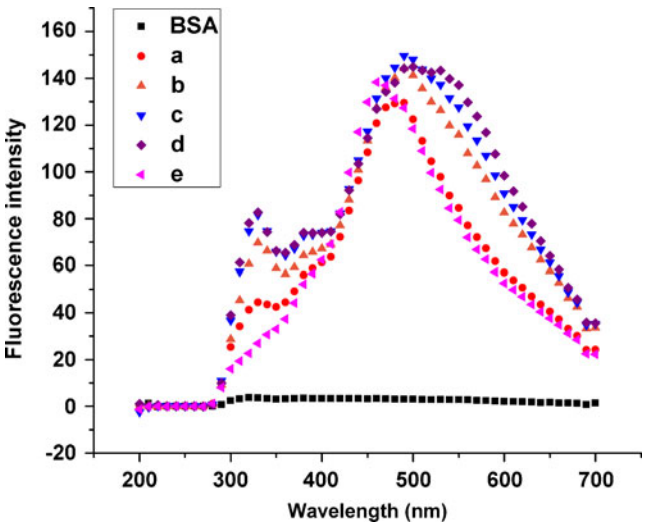

Fig. 5 Resonance Light Spectra (*bottom* to *top*) of BSA (1 mg/ml) and BSA (0.2, 0.4, 0.6, 1 mg/ml incubated with SNP ([SNP]=0.903×10^{-9} $molL^{-1}$)

Binding Constant (K) and Number of Binding Sites (n)

The number of binding sites (n) and the binding constant (K) between silver nanoparticle and BSA have been calculated using the Eq.8 for the quenching process [16]:

$$\log[(F_0 - F)/F] = \log K + n\log[Q] \quad (8)$$

A plot of log $[(F_0-F)/F]$ versus log [Q] gives a straight line, whose slope equals to n (the number of binding sites of SNP on BSA) and the intercept on Y-axis equals to log K.

Figure 6 depicts the double logarithm plots and Table 2 gives the corresponding results. The values of 'n' (Table 2) at the experimental temperatures were approximately equal to one which indicates that there is a single binding site in BSA for SNP which is independent of temperature in the range 277 K to 315 K.

Thermodynamic Parameters and Nature of Binding Forces

After calculating binding constant between BSA and SNP, we move towards characterization of thermodynamic forces responsible for binding between these two entities. The interaction forces originating from hydrogen bond, van der Waals, hydrophobic and hydrophilic interactions, electrostatic interaction etc. may exist between two molecules. Evaluation of parameters such as ΔH° and ΔS° of binding interactions enables us to determine the type of binding force.

If the enthalpy change (ΔH°) does not vary significantly over the temperature range studied, then the thermodynamic

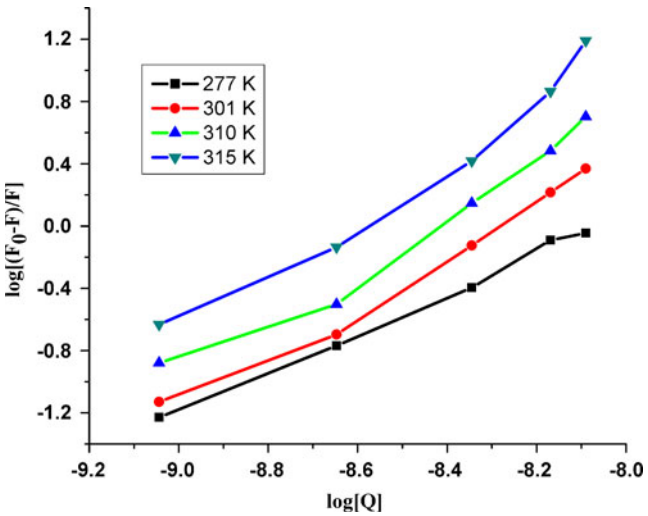

Fig. 6 Plots of the SNP quenching effect on BSA fluorescence at different temperature

Table 2 The binding parameters for the system of SNP–BSA

Temperature (K)	K ($Lmol^{-1}$)	n
277	1.716×10^{10}	1.2
301	1.812×10^{13}	1.5
310	1.512×10^{14}	1.6
315	1.068×10^{16}	1.8

parameters of ΔH° and ΔS° (entropy change) are determined using the vant Hoff Eq. 9:

$$\ln K = \frac{-\Delta H^\circ}{RT} + \frac{\Delta S^\circ}{R} \tag{9}$$

where K is the binding constant at the corresponding temperature. ΔH° and ΔS° are determined from the slope and intercept of linear vant Hoff plots. The Gibbs free energy (ΔG°) is estimated from the following equation

$$\Delta G^\circ = \Delta H^\circ - T\Delta S^\circ \tag{10}$$

According to the enthalpy and entropy changes, the model of interaction between SNP and biomolecule can be summarized as [17]: ΔH°>0 and ΔS°>0: indicative of hydrophobic forces; ΔH°<0 and ΔS°<0: indicative of van der Waals interactions and hydrogen bonds; ΔH°<0 and ΔS°>0: indicative of electrostatic interactions.

The regression of Eq. 9 yields the values of ΔH° and ΔS° to be 37.712 $kJmol^{-1}$ and 396.8 $Jmol^{-1}$ K^{-1} respectively. The values of thermodynamic parameter ΔG° are listed in Table 3. The negative sign for ΔG° indicates the spontaneity of the binding of silver nanoparticle to BSA. Here, we propose that the positive values of ΔH° and ΔS° show that the binding process is an entropy-driven and endothermic process. Endothermic and entropy-driven binding events are associated with the hydrophobic effect [17]. A hydrophobic interaction between BSA and SNP has also been reported by Ravindran et al. [18].Thus it can be concluded that hydrophobic forces play an important role in stabilizing the molecular complex.

Synchronous Fluorescence Spectra

Synchronous fluorescence spectra provide information on the molecular environment of the fluorophore functional group. The value of Δλ i.e. difference between excitation and emission wavelengths is an important operating parameter. According to Miller [19] when Δλ is 15 nm, synchronous fluorescence spectra indicates the changes in the microenvironment of tyrosine residues and when Δλ is 60 nm, it provides information on the microenvironment of tryptophan residues.

It can be seen from the Fig. 7a that when Δλ=60 nm there is a slight blue shift of approximately 2 nm in the emission wavelength of tryptophan residues and when Δλ= 15 nm, (Fig. 7b) there is no change in emission wavelength of tyrosine, only a gradual quenching is observed. This indicates that the microenvironment of tyrosine remains unaffected in the presence of SNP. The blue shift in the

Table 3 Thermodynamic parameters for BSA- SNP interactions

Temperature (K)	ΔG° ($kJ.mol^{-1}$)
277	−58.755
301	−83.115
310	−92.25
315	−97.325

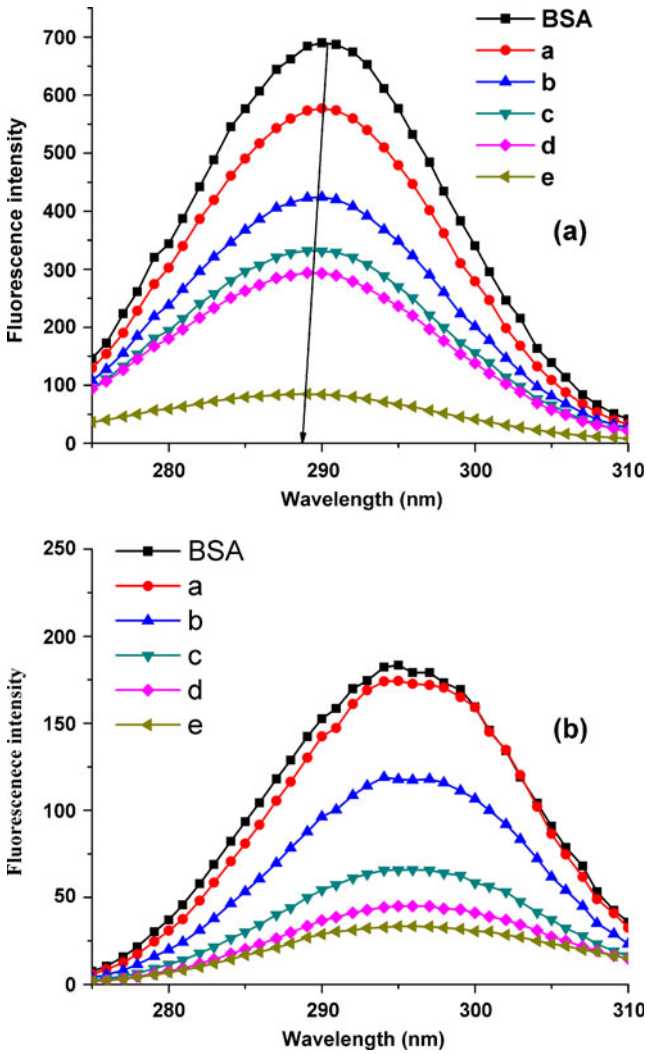

Fig. 7 **a** Synchronous fluorescence spectra at Δλ=60 nm, (*top* to *bottom*) 1 mg/ml BSA and 1 mg/ml BSA in presence of (a-e) 0.0903×10^{-9}, 0.225×10^{-9}, 0.451×10^{-9}, 0.677×10^{-9} and 0.8127×10^{-9} $molL^{-1}$ SNP. **b** Synchronous fluorescence spectra at Δλ=15 nm, (*top* to *bottom*) 1 mg/ml BSA and 1 mg/ml BSA in presence of 0.0903×10^{-9}, 0.225×10^{-9}, 0.451×10^{-9}, 0.677×10^{-9} and 0.8127×10^{-9} $molL^{-1}$

emission maxima of tryptophan indicates the shielding of the Trp residues from the aqueous phase i.e. an increase in the hydrophobicity around the Trp residues has occurred in the presence of SNP [20, 21].

Conclusion

The binding interactions of SNP with BSA were studied using fluorescence spectroscopy. BSA fluorescence is quenched by dynamic as well as static quenching processes. RLS spectra indicated the formation of a complex between BSA and SNP. The value of 'n'≈1 indicates the existence of a single binding site in BSA for SNP. The positive values of enthalpy and entropy change indicated that the interaction is mainly driven by hydrophobic forces. The process of binding is spontaneous as Gibb's energy change was negative. Synchronous fluorescence spectra indicate change in the microenvironment of tryptophan residues.

Acknowledgements We gratefully acknowledge the Department of Science and Technology (DST), Government of India, for their financial support through the DST INSPIRE - AORC scheme. We would also like to thank Mr. Narayan Karmakar, Project fellow, National Centre for Nanomaterials & Nanotechnology, University of Mumbai for the DLS spectrum.

References

1. Tian J, Wong K, Ho C, Lok C, Yu W, Che C, Chiu J, Tam P (2007) Topical delivery of silver nanoparticles promotes wound healing. Chem Med Chem 2:129–136
2. Li Y, Leung P, Yao L, Song QW, Newton E (2006) Antimicrobial effect of surgical masks coated with nanoparticles. J Hosp Infect 62:58–63
3. Furno F, Morley KS, Wong B, Sharp BL, Arnold PL, Howdle SM, Bayston R, Brown PD, Winship PD, Reid HJ (2004) Silver nanoparticles and polymeric medical devices: a new approach to prevention of infection? J Antimicrob Chemother 54:1019–1024
4. Naja G, Bouvrette P, Champagne J, Brousseau R, Luong J (2010) Activation of nanoparticles by biosorption for *E. coli* detection in milk and apple juice. Appl Biochem Biotechnol 162:460–475
5. Yang J, Wang H, Wang Z, Tan X, Song C, Zhang R, Li J, Cui Y (2009) Interaction between antitumor drug and silver nanoparticles: combined fluorescence and surface enhanced Raman scattering study. Chin Optic Lett 7:894–897
6. Shrivastava S, Bera T, Singh KS, Singh G, Ramchandrarao P, Dash D (2009) Characterization of antiplatelet properties of silver nanoparticles. ACS Nano 3:1357–1364
7. Evans TW (2002) Review article: albumin as a drug—biological effects of albumin unrelated to oncotic pressure. Aliment Pharmacol Ther 16:6–11
8. Lee PC, Meisel D (1982) Adsorption and surface enhanced Raman of dyes on silver and gold sols. J Phys Chem 86:3391–95
9. Xingcan S, Qi Y, Hong L, Haigang Y, Xiwen H (2003) Hysteresis effects of the interaction between serum albumins and silver nanoparticles. Sci China B 46(4):387–398
10. Liu X, Atwater M, Wang J, Huo Q (2007) Extinction coefficients of gold nanoparticles with different sizes and different capping ligands. Colloids Surf B Biointerfaces 58:3–7
11. Benesi HA, Hildebrand JH (1949) A spectrophotometric investigation of the interaction of iodine with aromatic hydrocarbons. J Am Chem Soc 71:2703–2707
12. Jhonsi MA, Kathiravan A, Renganathan R (2009) Spectroscopic studies on the interaction of colloidal capped CdS nanoparticles with bovine serum albumin. Colloids Surf B Biointerfaces 72:167–172
13. Lakowicz JR (1999) Principle of fluorescence spectroscopy, 3rd edn. Springer, New York
14. Huang CZ, Li YF, Li PF (2001) Determination of proteins by their enhancement of resonance light scattering by fuchsine acid. Fresenius J Anal Chem 371:1034–1036
15. Jiang XY, Li WX, Cao H (2008) Study of interaction between trans-resveratrol and BSA by the multispectroscopic method. J Solution Chem 37:1609–23
16. Kandagal PB, Ashoka S, Seetharamappa J, Shaikh SMT, Jadegoud Y, Ijare OB (2006) Study of the interaction of an anticancer drug with human and bovine serum albumin: spectroscopic approach. J Pharm Biomed 41:393–399
17. Ross DP, Subramanian S (1981) Thermodynamics of protein association reactions: forces contributing to stability. Biochemistry 20:3096–3102
18. Ravindran A, Singh A, Raichur AM, Chandrasekaran N, Mukherjee A (2010) Studies on interaction of colloidal Ag nanoparticles with Bovine Serum Albumin (BSA). Colloids Surf B Biointerfaces 76:32–37
19. Miller JN (1979) Proc Anal Div Chem Soc 16:203
20. Liu Q, Xu X, Xie Y (2001) Synchronous fluorescence spectra of fibrinolytic principle from snake venom of Agkistrodon Acutus. Spectros Lett 34:427–425
21. Zhang Y, Zhou B, Liu Y, Zhou C, Ding X, Liu Y (2008) Fluorescence study on the interaction of bovine serum albumin with P- aminoazobenzene. J Fluoresc 18:109–118